Adhesive bonded Structures – A life in the light of continuum mechanics?

St. Froemmel [a] and H.-J. Gudladt [b]

Institute for Materials Science, Universitaet der Bundeswehr Muenchen,

Werner-Heisenberg-Weg 39, 85577 Neubiberg, Germany,

[a] stephan.froemmel@unibw.de, [b] hans-joachim.gudladt@unibw.de

Keywords: Adhesion, adhesive, continuum mechanics, quasi-static, fatigue, aluminium, epoxy, laser treatment, S-N-curve, shear strength, lifetime, fracture mechanics

Abstract

Adhesive bonding is one of the best appliances to solve material depended joining problems. To utilise the profits of adhesive bonding technology the characteristic mechanical behaviour of structural bonding has to been known. For the experiments an aluminium alloy and a 2k-epoxy adhesive have been selected. The aluminium surface has been activated by NdYAg laser treatment either completely or partially by a characteristic line pattern. The surfaces have been characterised by SEM. The 2k-adhesive system was mixed in a double-centrifugal mixing machine under vacuum conditions. After curing at defined temperature and time, tension tests under quasi-static loading conditions undertaken with the lap shear specimens have shown that the strength depends on the degree of the laser-activated specimen surface. Areas that were totally activated by the laser beam induce the highest shear strength for the lap shear specimens. The surface treatment influences the fatigue tests as well. Accordingly, a lower degree of activation creates lower lifetimes. Furthermore, the testing frequency of the used resonance pulsing test machine decreases during progressive life time caused by sample stiffness reduction. This could be interpreted as a proceeding damage process. The latter can be discussed in the light of fracture mechanics.

Introduction

Light weight construction is a powerful industrial attempt for structural components in vehicles as airplanes, trains or cars. Therefore, a combination of different materials (metal, glass, plastics) has to be used. Adhesive bonding is one of the best appliances to solve material depended joining problems. To utilise the profits of adhesive bonding technology the characteristic behaviour of structural bonding e.g. strength, fatigue, damage qualities, or ageing, has to been known.

From the aspect of damage, a good bonding depends on the kind of defects, created prior or during the curing process. Therefore an optimized surface treatment and also a good adhesive preparation is necessary. Laser treatment is one of the most effective surface preparation techniques which can be used for cleaning and activating different materials e.g. metals, plastics, ceramics, etc. before adhering or painting [1–12]. Consequently, it has been used for preparing the samples´ surfaces.

Experimental Section

Materials and preparation. For the experiments the simple specimen type of single overlap lap shear samples according to DIN 1465 had been chosen [13]. The adherents are 100mm long, 25mm wide and have a thickness of 3.6mm. The surface to be bonded is 12.5mm long and 25mm wide. The thickness of the bondline is 0.1mm. The adherent was manufactured from the aluminium alloy AW 6156-T4 (Table 1) in the institute. This alloy was developed for aircraft constructions [14,15].

The used adhesive was the cold-setting, 2-part epoxy system Hysol EA9394 which is certified for aircraft applications. It is filled with aluminium powder for better performance in interaction with metallic adherents (Table 2).

Table 1. Composition and mechanical parameters of the used aluminium alloy

aluminium alloy AW 6156-T4	
Al [%]	96.7
Cu [%]	0.97
Si [%]	0.80
Mg [%]	0.69
Mn [%]	0.48
UTS, R_m [MPa]	328
$R_{P0.2}$ [MPa]	231
E-Modulus [GPa]	74

Table 2. Specific data of the used epoxy adhesive system

2-part epoxy adhesive Hysol EA9394	
filler	Al-powder (35%)
curing conditions	1000min at 66°C
glass transition temperature	90°C (dry)

To obtain a realistic result of mechanical properties that contains a failure probability, the whole sample preparation must be done in a repeatable way. Instead traditional methods e.g phosphoric acid anodisation (PAA) a NdYAg marking laser induced thermal oxidation process was used as activating method of the aluminium surface. During this process the upper surface layer of the adherent is molten and solidificated rapidly, thereafter. Therefore, a distinctive surface topology was made. In the area of the laser beam focus the surface is valley like. A hill structure has been found where two small ridges had been cumulated (Fig. 2-4) [16].

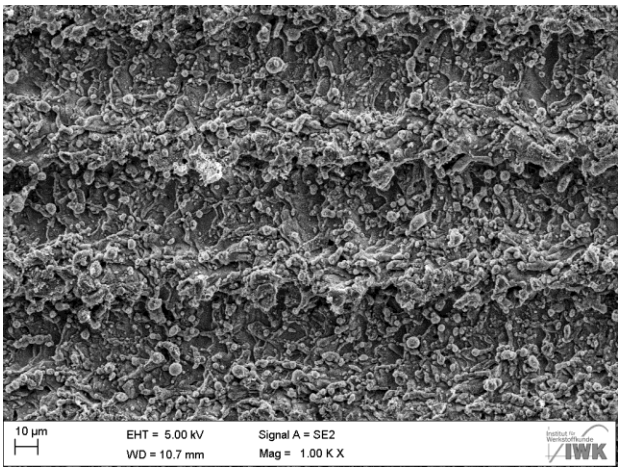

Fig.2 (left). SEM picture of a laser treated aluminium surface with hill and valley structure

Fig.3 (below, left). SEM picture of bead structure on the thermal oxidized aluminium surface

Fig.4 (below, right). Detailed SEM picture of the solidificated bead of melted aluminium on the surface

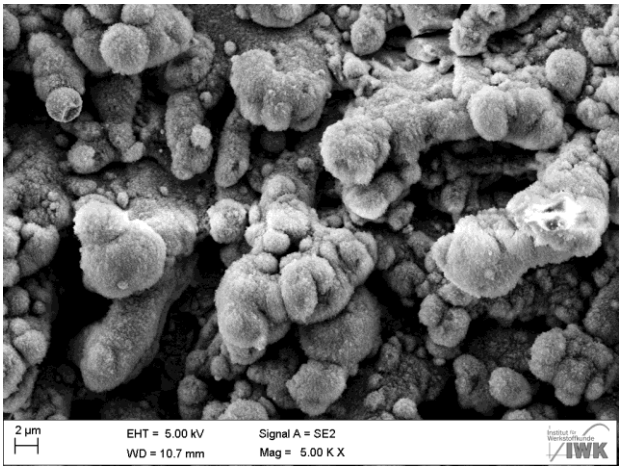

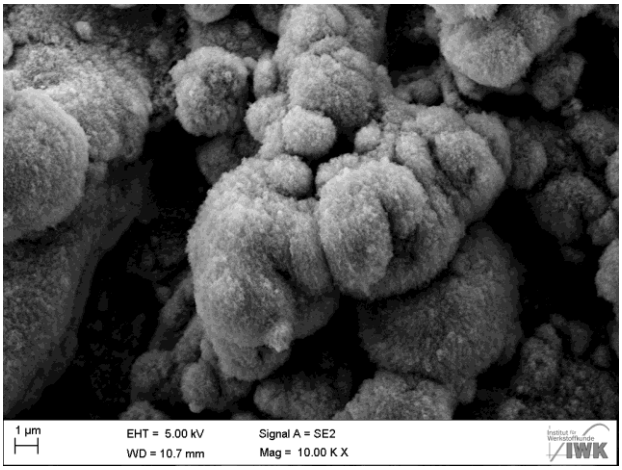

The laser lines were aligned in force direction of the mechanical tests and the activated area was varied between 100% and 0% by modifying the distance between two parallel laser beam lanes.
The two parts of the epoxy adhesive system were mixed under low pressure of about 30mbar in a double-centrifugal mixing equipment. A comparison of some usual mixing technologies showed a decrease of number and size of voids. This mixing method causes a homogenous adhesive without any detectable voids greater than 10µm. In this case, tensile tests showed an improvement of lap shear strength and cyclic lifetime [16]. After laser treatment substrates were coated with the adhesive and then joined under pressure to a defined bondline thickness of 100µm. The adhesive was cured for 60 minutes at room temperature followed by a further curing step at 66°C for 1000 minutes. Afterwards, the samples were stored at room temperature for 24 hours before testing.

Testing conditions. The samples were tested under static loading conditions with a class 1 electro-mechanical testing machine. The strain values had been measured with a class 0.5 extensometer. Furthermore, fatigue tests had been undertaken with the lap shear samples at a positive mean stress (R_F=0.1). As testing equipment for lifetimes lower than 10000 cycles (LCF) a servohydraulic load frame and for lifetimes up to 10 million cycles (HCF) a resonance pulsing machine had been used. The resonance frequency of the samples was about 140Hz, decreasing with developing damage of the sample [16]. The servohydraulic testing machine operates with a constant frequency of 1Hz. All tests were carried out at 25°C and about 50% relative moisture. Because of the open biaxial stress condition inside the bondline that depends on the kind of specimen in the following only the applied force, *F*, has here used for all further calculations.

Results

Quasi-static loading conditions. Tension tests under quasi-static load showed that the lap shear strength depends directly on the degree of the activated area. The degree of this area depends on the number of lines on the substrate surface created by the laser beam. Slightly overlapping lines were denoted as completely activated samples. Consequently, the highest lap shear strength, F_{Break}, had been found at these samples. In Fig. 4, the lap shear strength is plotted against the degree of laser activation. For samples with greater distances between the laser lines the lap shear strength decreases. The lowest strength was found at samples without any laser treatment. Within the error bars, a linear regression shows a good correlation (red line in Fig. 4, R^2=0.964)). Taking a rule of mixture into account one obtains the black dashed line. For this purpose the upper and lower mean value $F_{Break}^{0\%}$ and $F_{Break}^{100\%}$ had been weighted by the laser activated area, α, (Eq. 1, black dashed line in Fig. 4).

$$F_{Break} = F_{Break}^{0\%} \cdot \alpha + F_{Break}^{100\%} \cdot (1 - \alpha) \quad (1)$$

Additionally to the standard deviation of the measurements shown in Fig. 4 all data obtained from the seven different activated areas were analyzed in a statistical manner by using a Weibull approach [17,18] as shown in Fig. 5 exemplary for the totally activated (red dots) and non-activated (blue circles) samples. The failure probability, P_F, is calculated from F_{Break} by equation 2, where F^* represents the maximum of the density function at a failure probability, P_F, of 63.2% and m the Weibull exponent, respectively.

$$P_F = 1 - e^{\left\{-\left(\frac{F_{Break}}{F^*}\right)^m\right\}} \quad (2)$$

Taking m and F^* as characteristic parameters to determine the strength of the adhesive bonded structure, one obtains Fig. 6, where these parameters are plotted versus the laser activated area. The

lowest value of the location parameter, F^*, is displayed by the non-activated and the highest one by fully activated samples. The values in this plot show a linear dependence on the degree of the laser activated area with a correlation of R^2=0.984 (see also F_{Break} in Fig. 4). The Weibull exponent, m, a degree of the variation of sample failure varies between 8 and 10 for non-activated samples and those ones with about 50% activated area. It increases up to 20 for totally activated samples. Consequently, the latter show the lowest scatter in lap shear strength.

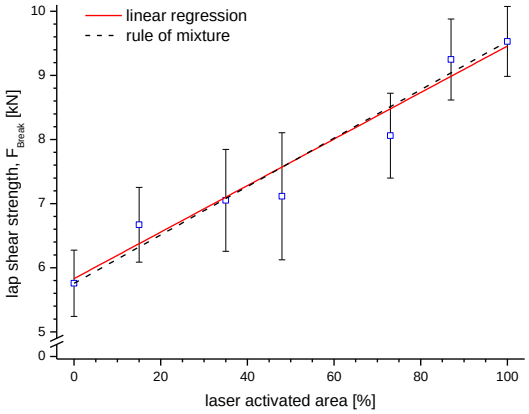

Fig.4 (left). Mean lap shear strength and variance of samples with varied activated areas, appliance of linear regression and rule of mixture

Fig.5 (below, left). Weibull plot of lap shear strengths of totally activated and non-activated samples

Fig.6 (below, right). Weibull exponent m and maximum value, F^*, of different activated samples

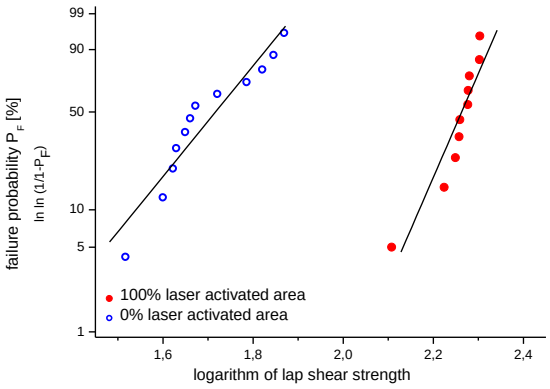

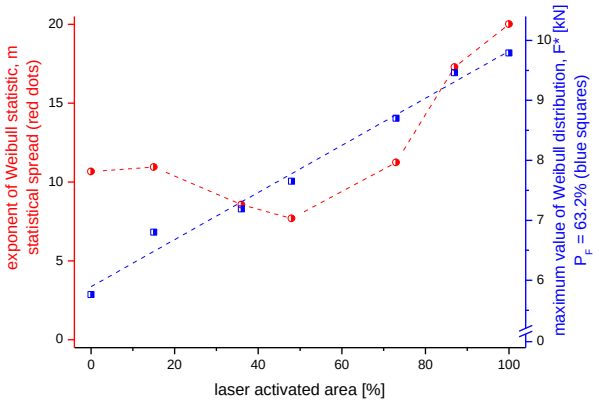

Cyclic loading conditions. In case of fatigue tests, the maximum load, F_{Max}, was varied between 1.3 and 8.0kN. The S-N-curve in Fig. 7 has been plotted in a log-log presentation [19–22] as follows:

$$\log F_{Max} = b \cdot \log N_f + a \qquad (3)$$

where a and b were denoted as intercept and Basquin-like exponent.
For a given F-value, higher activated samples reach longer lifetimes under cyclic loading conditions. Fig. 8 displays the inverse Basquin-like exponent, b, and the intercept, a, of the S-N-curves plotted versus the activated area. The exponent increases slightly from -0.10 to -0.08. The intercepts increase from 1.8 for non-activated samples to 2.5 for samples with 100% activation. Between 40% and 70% activated area the intercept was found to the constant at (2.15±0.05)kN.

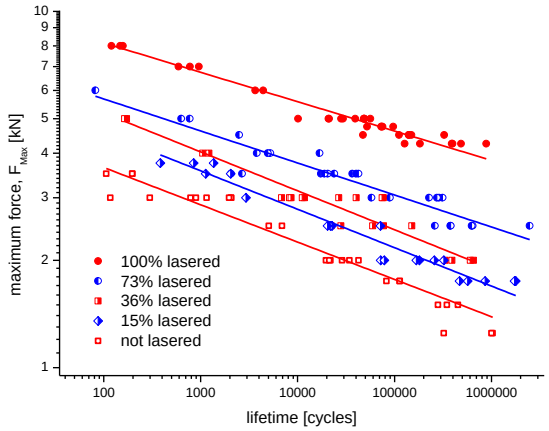

Fig.7. S-N-curve (R=0.1) of sample lifetime for different activated

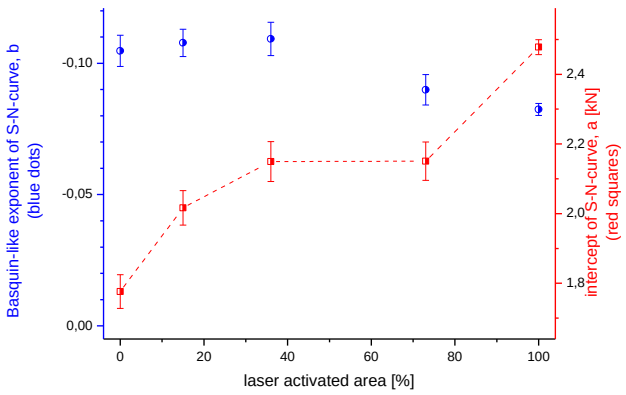

Fig.8. Demonstration of inverse Basquin-like exponents and intercepts of S-N-curve (Fig.7)

Similar to the static tests, all data have been collected and analysed in a statistical manner. Starting from this one can use the following equation:

$$P_F(F_{Max}, N = const.) = 1 - e^{\left\{-\left(\frac{F_{Max}}{F^*}\right)^k\right\}} \quad (4)$$

where F_{Max}, F^*, and κ represent the highest force, the maximum of the density function (P_F=63.2%), and the Weibull exponent. Taking a constant lifetime of N=10^6 cycles, the corresponding F_{Max}-values can be calculated by using Eq. 3. Finally, Fig. 9 shows $P_F(FMax)$ in a Weibull presentation. The loads of non-activated samples were found between 1.1 and 1.6kN and between 3.4 and 4.2kN for those ones with a totally activated area. A numerical regression that based on the Weibull distribution (black line) shows a good agreement with the experimental data.

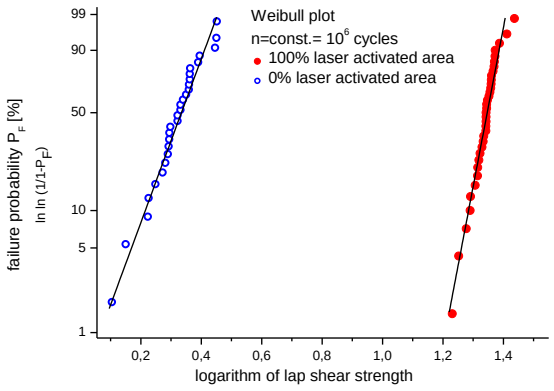

Fig.9. Weibull plot of failure probability of transformed data at constant lifetime of one million cycles versus the logarithm of lap shear strength

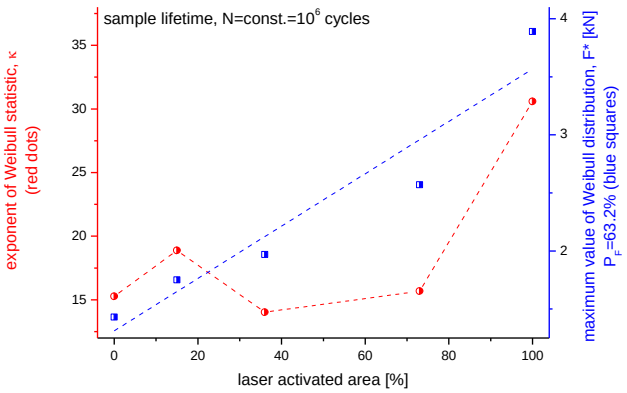

Fig.10. Exponent and maximum value of Weibull statistic (Fig. 9) versus laser activated area

In Fig. 10 κ and F^* were displayed against the laser activated area. The κ value of the Weibull distribution remains about 15 up to a laser activating level of 70%. Therefore, it rises to 30 for totally activated samples. F^* increases with increasing activating level from 1.5 to 3.3. Hence, samples with a greater activated area fail at higher loads than those with lower ones. A linear fit of these data by using a simple rule of mixture cannot be found.

Discussion

The presented experiments illustrate the improvement of mechanical properties for adhesive bonded structures by laser activation of the aluminium surface. Tensile tests under quasi-static as well as under cyclic loading conditions undertaken with surface treated and adhesive bonded single overlap samples showed that they failed in two different ways. Samples with a totally laser activated area failed in a cohesive manner by destroying the bond line. At samples with non-activated surface the interface between adhesive and adherent failed. Samples with partially activated surface failed in a cohesive and adhesive mixed manner. Within the laser lines the crack propagates near the interface in a cohesive manner. Between the laser lines the activation is less pronounced and, consequently, the interface initials the crack leading to an adhesive fracture. Furthermore, under monotonic loading condition the lap shear strength, F, as a function of the degree of activation has a constant slope (see Fig. 4) and decreases with decreasing laser treatment. This behaviour can be simulated with the physical approach by using the "rule of mixture" (Fig. 4, 5). The latter takes cohesive and adhesive fracture into account. The lower bound, F_{Min}, is given by an adhesive failure whereas the upper bound, F_{Max}, by a cohesive one. In most cases, the mechanical behavior of bonded structures has been discussed in the light of continuum mechanics. However, details of the failure of bonded structures can be explained more easily by the linear-elastic fracture mechanics (LEFM). Taking a damage model in account, the failure depends on the defect spectrum [23]. The spectrum depends on the kind of laser treatment. The failure probability corresponds to the kind of defect, a, and can be described by a Weibull distribution. A possible solution could be found in the approach of fracture mechanics. In this connection, the dispersion of efficiency of the existing defect, a, appoints the performance of sample in the following way [24]:

$$P(a) = e^{\left\{-\left(\frac{a}{a^*}\right)^{-\gamma}\right\}} \tag{5}$$

where a and γ are the efficiency of defects and distribution exponent. Taking the LEFM into account for a given stress intensity $K = \frac{F}{A} \cdot \sqrt{\pi \cdot a}$ where A is denoted as area of the overlap one obtains Eq. 6:

$$P_S(F) = e^{\left\{-\left(\frac{F}{F^*}\right)^{k}\right\}} \tag{6}$$

Consequently, the fracture of the bonded structure depends on a critical stress or force ($F^* = F_{Break}$) and the failure probability can be described by using a Weibull statistic (Fig. 5, 6). Large scatter in F_{Break} at samples with adhesive failure reflects in a small Weibull exponent (m<10). Whereas in case of low scatter in F_{Break} detected at cohesive-failed samples the Weibull exponent becomes higher than 10 (Fig. 6). The latter reflects in the fatigue data (Fig. 10, 11), too. In this case, the exponent was found to be 15 and 30, respectively.

Conclusion

Experiments showed that laser treatment is a good alternative method for surface preparation before bonding. The influence of the degree of laser treatment on the lap shear strength has been presented. The results obtained under static loading conditions follow a simple rule of mixture. However, the rule of mixture becomes non-linear in case of cyclic deformation. That may depend on differences in the fatigue crack initiation. Taking LEFM into account the fracture of adhesive bonded specimens and its dependence on the degree of laser treatment is explainable. The divergence of experimental fatigue data to the rule of mixture should be higher for samples with different activating geometries. Adequate tests are in progress. Furthermore, a well-grounded analysis of experimental data and its handling for engineering application has to be based on an established statistical approach.

Acknowledgement.

The authors wish to thank Dr. Baer for SEM analysis and fruitful discussions.

References

[1] J. Heitz, Enhanced adhesion of metal-films on pet after UV-laser treatment, Appl Phys A-Mater 55 (1992) pp.391–392

[2] H. Dodiuk, A. Buchmann, S. Kenig, M. Rotel, J. Zahavi, T. Reinhart, Preadhesion laser treatment of aluminum surfaces, J Adhesion 41 (1993) pp.93–112

[3] A. Buchman, Laser-induced adhesion enhancement of polymer composites and metal-alloys, J Adhes Sci Technol 8 (1994) pp.1211–1224

[4] Z. Gendler, A. Rosen, M. Bamberger, M. Rotel, Improvement of adhesive bonding strength in sealed anodized aluminium through excimer laser prebond treatment, J Mater Sci 29 (1994) pp.1521-1526

[5] G.W. Critchlow, D.M. Brewis, D.C. Emmony, C.A. Cottam, Initial investigation into the effectiveness of CO2-laser treatment of aluminium for adhesive bonding, Int J Adhes Adhes 15 (1995) pp.233-236

[6] M. Murahara, Photochemical surface modification of polypropylene for adhesion enhancement by using an excimer laser, J Adhes Sci Technol 9 (1995) pp.1593–1599

[7] M. Rotel, Preadhesion laser surface treatment of carbon fiber reinforced PEEK composite, J Adhesion 55 (1995) pp.77-97

[8] A. Hartwig, G. Vitr, S. Dieckhoff, O.-D. Hennemann, Surface treatment of an epoxy resin by CO_2 laser irradiation, Angew Makromol Chem (1996) pp.177–189

[9] E. Moosbrugger, Ermittlung werkstoffspezifischer Prozessparameter für die Vorbehandlung von Kunststoffoberflaechen mit Laserstrahlen zur spaeteren Verklebung: [Schlussbericht ; Abschlussdatum des Vorhabens: Mai 1995], Robert Bosch Zentralbereich Forschung und Vorrausentwicklung Abt. Kunststoffe, Waiblingen, 1996

[10] P.E. Lafargue, The laser ablation/desorption process used as a new method for cleaning treatment of low carbon steel sheets, Surf Coat Tech 106 (1998) pp.268–276

[11] P. Laurens, B. Sadras, F. Decobert, F. Arefi-Khonsari, J. Amouroux, Enhancement of the adhesive bonding properties of PEEK by excimer laser treatment, Int J Adhes Adhes 18 (1998) pp.19-27

[12] R. Rechner, I. Jansen, E. Beyer, Influence on the strength and aging resistance of aluminium joints by laser pre-treatment and surface modification, Int J Adhes Adhes 30 (2010) pp.595–601

[13] DIN 1465, Klebstoffe - Bestimmung der Zugscherfestigkeit von Ueberlappungsklebungen

[14] P. Leque, P. Lassince, Aluminum alloy development for the airbus A380 - part 1, AMP (2007) pp.33–35

[15] P. Leque, P. Lassince, Aluminum alloy development for the airbus A380 - part 2, AMP (2007) pp.41–44
[16] H.-J. Gudladt, S. Froemmel, Damage behaviour of bonded structures under static and cyclic loading conditions, in: J. Wellnitz (Ed.), Sustainable automotive technologies 2010: Proceedings of the 2nd international conference, Springer, Berlin, Heidelberg, 2010, pp. 191–197
[17] W. Weibull, A statistical distribution function of wide applicability, J Appl Mech-T ASME (1951) pp.293–297
[18] W. Weibull, Discussion of: A statistical distribution function of wide applicability, J Appl Mech-T ASME (1952) pp.233–234
[19] A. Woehler, Ueber die Versuche zur Ermittlung zur Ermittlung der Festigkeit von Achsen, welche in den Werkstätten der Niederschlesisch-Maerkischen Eisenbahn zu Frankfurt a.d.O. angestellt sind., Zeitschrift für Bauwesen 13 (1863) pp.233–258
[20] A. Woehler, Resultate der in der Zentralwerkstatt der Niederschlesisch-Maerkischen Eisenbahn zu Frankfurt a.d.O. angestellten Versuche über die relative Festigkeit von Eisen, Stahl und Kupfer., Zeitschrift für Bauwesen 16 (1866) pp.67–84
[21] A. Woehler, Ueber die Festigkeitsversuche mit Eisen und Stahl., Zeitschrift für Bauwesen 20 (1870) pp.73–106
[22] O. Basquin, The exponential law of endurance tests, ASTM Proceedings 10 (1910) pp.625–630
[23] J. Baer, W. Berger, H.-J. Gudladt, Damage behaviour of an Al_2O_3 particle-reinforced 6061 alloy induced by monotonic and cyclic deformation, Zeitschrift für Metallkunde 97 (2006) pp.336-343
[24] R. Schubert, H.-J. Gudladt, K. Heckel, Der statistische Groesseneinfluss bei UDIMET 700 (PM) AS HIP, Proceedings of Werkstoffwoche 96, Stuttgart (1996)